ARTICLE

Interaction between Potassium Phosphate Buffer Solution and Modeling Cell Membrane Investigated by Sum Frequency Generation Vibrational Spectroscopy†

Weilai Yang, Kangzhen Tian, Shuji Ye*

Hefei National Laboratory for Physical Sciences at the Microscale and Department of Chemical Physics and Synergetic Innovation Center of Quantum Information and Quantum Physics, University of Science and Technology of China, Hefei 230026, China

(Dated: Received on April 14, 2015; Accepted on May 7, 2015)

Potassium phosphate buffer solution has been widely used in the biological experiments, which represents an important process of the interaction between ions and biomolecules, yet the influences of potassium phosphate on biomolecules such as the cell membrane are still poorly understood at the molecular level. In this work, we have applied sum frequency generation vibrational spectroscopy and carried out a detailed study on the interaction between potassium phosphate buffer solution (PBS) and negative 1,2-dimyristoyl-d54-sn-glycero-3-[phospho-rac-(1-glycerol)] (d_{54}-DMPG) lipid bilayer in real time. The PBS-induced dynamic change in the molecular structure of d_{54}-DMPG lipid bilayer was monitored using the spectral features of CD_2, CD_3, lipid head phosphate, and carbonyl groups for the first time. It is found that K^+ can bind to the cell membrane and cause the signal change of CD_2, CD_3, lipid head phosphate, and carbonyl groups quickly. Potassium PBS interacts with lipid bilayers most likely by formation of toroidal pores inside the bilayer matrix. This result can provide a molecular basis for the interpretation of the effect of PBS on the ion-assisted transport of protein across the membrane.

Key words: Sum frequency generation, Potassium phosphate buffer, Lipid bilayer, Toroidal pore, Interaction

I. INTRODUCTION

Cell membranes are an important component of the machinery of life. They not only work as a barrier to separate the interior of all cells from the outside environment, but also regulate many biological activities and functions such as ion transport, signal regulation, immune response, and membrane assembly [1], which strongly depend on their structural and dynamical properties. Small changes in the conformation and the electrical properties of the membrane surface can have a large impact on the physiological and biochemical properties of the membrane [2, 3]. In addition, the fluid at the cell membrane boundary is a salt solution containing a variety of ions, rather than pure water [4]. The properties of aqueous solutions at the membrane interface can largely influence the structural and dynamical properties of cell membranes and thus affect their functions [1]. Therefore, it is very important to understand the interaction between the salt solutions and the cell membranes. A large number of experimental, computational, and theoretical studies have been performed to investigate the ion-membrane interactions [5−11]. Despite substantial progress, many issues remain unresolved. Understanding the character of aqueous solutions at their interface with biological membranes has been considered to be critical to the research progress on many fronts [1].

Potassium ion is the most abundant cations in the human body [12]. In addition, phosphate ion is one of the important anions present in the intracellular and extracellular fluid [13, 14]. It can form strongly hydrogen-bonded and salt-bridged complexes with arginine and lysine to activate the voltage gated channel protein [15−18]. Recently, Ye *et al.* applied sum frequency generation vibrational spectroscopy (SFG-VS) to investigate the interactions between peptide mastoparan (MP) and neutral phosphocholine lipid bilayers with the presence of phosphate anions and observed that phosphate ions can greatly promote the association of MP with lipid bilayers. In phosphate buffer solution (PBS), MP can insert not only into negatively and neutrally charged lipid bilayers, but also into positively-charged lipid bilayer [19]. The presence of phosphate anions can surprisingly overcome the hydrophobic mismatching ef-

†Dedicated to Professor Qing-shi Zhu on the occasion of his 70th birthday.

*Author to whom correspondence should be addressed. E-mail: shujiye@ustc.edu.cn, FAX: +86-551-63603462

fects, leading to the insertion of MP into lipid bilayers with much longer hydrophobic length [20]. Although potassium PBS has been widely used in many biological experiments, the influences of potassium phosphate on the cell membrane are still poorly understood at the molecular level. A molecular level elucidation of the dynamics process on the interaction between potassium PBS and membrane will not only improve our current knowledge about the ion-membrane interaction itself but also aid in understanding the behavior and process with which cell membrane is associated.

Negatively charged membranes play important roles in many biological processes. As the first step of a series of systematic study, here we chose negative 1,2-dimyristoyl-d54-sn-glycero-3-[phospho-rac-(1-glycerol)] (d_{54}-DMPG) as model and carried out a detailed study on the interaction between potassium PBS and d_{54}-DMPG lipid bilayer in real time. Planar substrate-supported lipid bilayer has been widely used as a model to mimic the cell membrane [21]. SFG-VS is a versatile and powerful spectroscopic tool that permits to identify interfacial molecular species and determine the orientation information of the interfacial functional groups *in situ* in real time [22−26]. It has been applied to elucidate the influence of ions on the structures, hydration states, and orientation of the Langmuir monolayer [27]. DMPG is used because phosphatidylglycerols (PG) are the most abundant negative lipids in the plasma membrane of microorganisms and the chloroplast membrane of plants [3, 28].

II. EXPERIMENTS

A. Materials and sample preparations

d_{54}-DMPG lipids were purchased from Avanti Polar Lipids (Alabaster, AL). Chemical structure of d_{54}-DMPG is shown in Fig.1. The potassium salts KH_2PO_4 and K_2HPO_4 were ordered from Aldrich with a purity >99.8%. Right-angle CaF_2 prisms were purchased from Chengdu Ya Si Optoelectronics Co., Ltd. (Chengdu, China). All of the chemicals were used as received. The salts were baked for more than 6 h to remove the organic impurities. The potassium PBS with a pH of ∼7 was prepared by dissolving KH_2PO_4 and K_2HPO_4 into ultrapure water from a Milli-Q reference system (Millipore, Bedford, MA). d_{54}-DMPG was dissolved in mixed solvents of chloroform and methanol (Sinopharm Chemical Reagent Co., Ltd.) in term of the proportion of 2:1 and kept at −20 °C.

CaF_2 prisms were thoroughly cleaned using a procedure with several steps. At first they were soaked in toluene for at least 24 h and then sonicated in soap detergent solution for 0.5 h. After that, they were rinsed with deionized (DI) water before soaking in methanol for 10 min. All of the prisms were then rinsed with an ample amount of DI water and cleaned inside Harrick plasma chamber for 10 min immediately before depositing lipid molecules on them. Substrates were tested using SFG and no signal from contamination was detected.

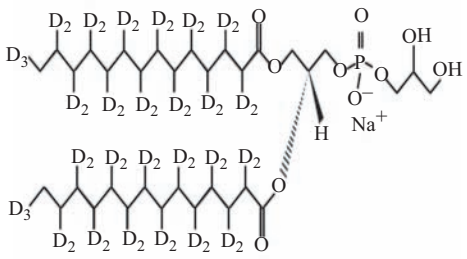

FIG. 1 Chemical structure of d_{54}-DMPG.

Lipid bilayer was prepared on CaF_2 substrates using Langmuir-Blodgett (LB) and Langmuir-Schaefer methods with a KSV mini trough LB system. Ultrapure water was used throughout the experiments for bilayer preparation. The detailed procedure was similar to previous reports [19, 20]. The bilayer was immersed in water inside 2-mL reservoir throughout the entire experiment. The same ionic intensity potassium salts were injected into reservoir for potassium salt-bilayer interaction experiments.

B. SFG-VS experiments

Details regarding SFG theories and instruments have been reported previously [22−27]. The SFG setup is similar to that described in our earlier work [29, 30]. In this work, all the experiments were carried out at the room temperature (24 °C). SFG spectra from lipid bilayer with different polarization combination including ssp (s-polarized SFG output, s-polarized visible input, and p-polarized infrared input) were collected using near total internal reflection. All SFG spectra were averaged over 100 times at each point and normalized by intensities of the input IR and visible beams.

III. RESULTS AND DISCUSSION

A. The influence of PBS on the tailed groups of d_{54}-DMPG bilayer

SFG has been applied to study the interaction between PG model cell membrane and nanoparticles [31] or peptides [32−34]. Generally, the ssp spectra of PG lipid are dominated by several peaks at ∼2850, ∼2875, ∼2920, and ∼2940 cm^{-1} [35]. The peaks at ∼2850 and ∼2875 cm^{-1} are assigned to the CH_2 symmetric and CH_3 symmetric stretches of tailed groups, respectively. But the ∼2920 cm^{-1} peak may originate from the asymmetric stretch of CH_2 group or the symmetric stretch of the DMPG glycerol moiety. The ∼2940 cm^{-1} peak

DOI:10.1063/1674-0068/28/cjcp1504070

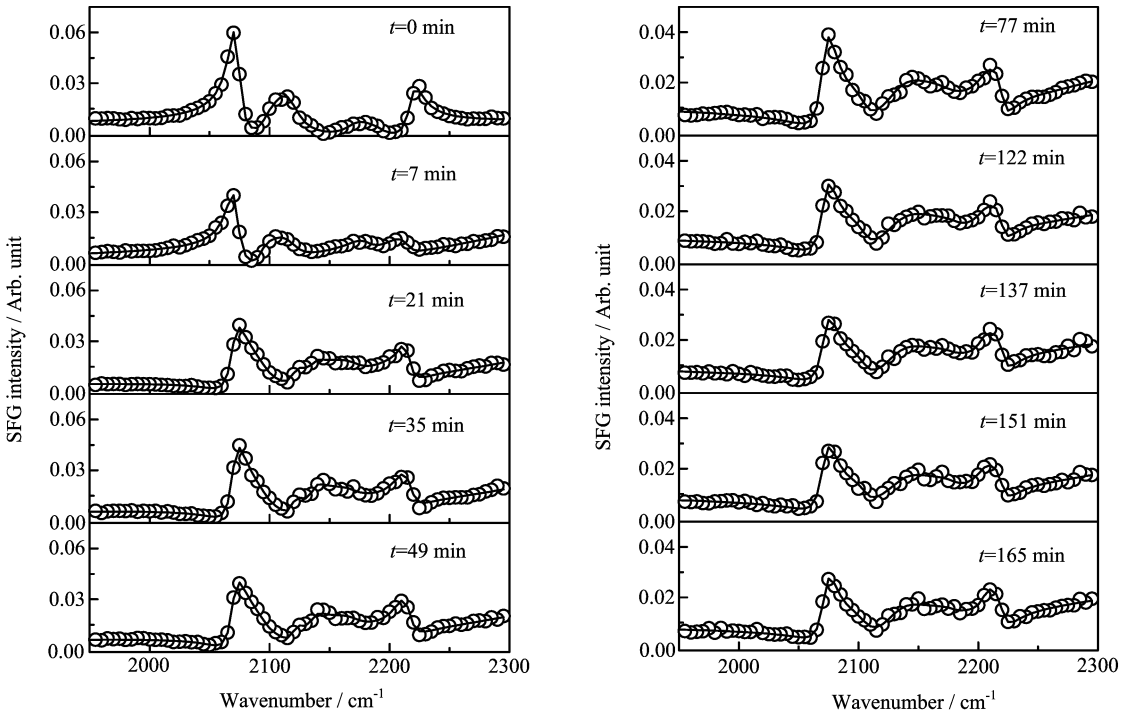

FIG. 2 Time dependence of ssp CD region spectra after adding PBS (0.5 mol/L, 40 μL) into the d_{54}-DMPG bilayer subphase at t=0 min. The spectra at t=0 min was collected in DI water. Open circles show the experimental data, solid lines represent the fitting profile.

is a combination of CH_3 Fermi resonance, CH_3 asymmetric stretch and stretching of the PG glycerol moiety [36−38]. To avoid the signals from the head group, here we studied the deuterated DMPG (d-DMPG) instead of DMPG. The hydrocarbon interior of d-DMPG is deuterated while its head glycerol group is hydrogenated. Therefore, we can distinguish the behaviors of lipid head and tailed CD_3 group [39, 40].

Figure 2 presents the dynamic spectra of the d-DMPG tailed groups in frequency range from 1950 cm^{-1} to 2300 cm^{-1} after adding 40 μL PBS (0.5 mol/L) to get a target ionic strength of 20 mmol/L. Before injecting PBS, the spectra at t=0 min are dominated by four peaks at ∼2070, ∼2115, ∼2170, and 2220 cm^{-1}, which are contributed by the CD_3 symmetric stretch (CD_3ss), CD_3 Fermi resonance (CD_3 Fermi), CD_2 Fermi resonance (CD_2 Fermi), and CD_3 asymmetric stretch (CD_3as), respectively [41−44]. The signals from the proximal leaflet and distal leaflet of d_{54}-DMPG bialyer can't cancel each other effectively because of the electrostatic repulsion between d_{54}-DMPG molecules, giving rise to obvious SFG signals from the tailed groups. Following the addition of the PBS solution (0.5 mol/L, 40 μL), obvious change in the SFG spectra profile is observed between 0 and 21 min, indicating PBS interacts with d_{54}-DMPG bilayer rapidly. After then, the spectra change very slowly. To quantitatively analyze the change in the intensity of SFG peaks, we fitted the spectra using a standard procedure, Eq.(S2) in supplementary material.

Figure 3(a) plots the fitting CD_3ss and CD_3as strength as a function of time. After injecting PBS solution, the fitting CD_3ss and CD_3as strength changes very small. It is well known that the change in intensity arises from the change of the orientation or the symmetry [22−27]. To further look insight into the influence of the ions on the lipid chains, we estimated the orientation angle (θ_{chain}) of the lipid chains according to a relationship of θ_{chain}=41.5−θ_{CD_3} [45]. Here θ_{CD_3} is the orientation angle of the end CD_3 group, which can be roughly determined using a common procedure in term of the intensity ratio of $\chi^{(2)}_{ssp}(CD_3as)/\chi^{(2)}_{ssp}(CD_3ss)$ (Fig.3(b)) [45]. The detailed formulas and procedure on the determination of the orientation of CD_3 were put in the supplementary material (Fig.S1). The resulted θ_{chain} is plotted as a function of time in Fig.3(c). As shown in the Fig.3(c), after injecting PBS, θ_{chain} increases quickly and then remains almost constant. It may indicate the interaction between PBS solution and lipid bilayer is very fast, which is further confirmed by the change of the head groups discussed below.

B. The influence of the PBS on the head groups of d_{54}-DMPG bilayer

After understanding the influence of PBS on the tailed group of d-DMPG bilayer, we turned to investi-

DOI:10.1063/1674-0068/28/cjcp1504070

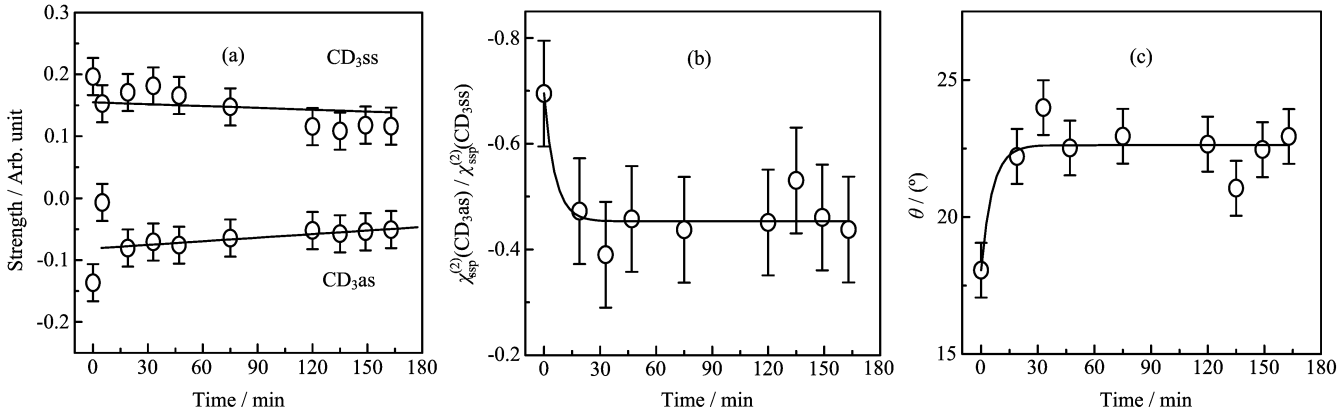

FIG. 3 (a) Time dependence of ssp CD_3ss and CD_3as fitting strength, (b) the ratio $\chi^{(2)}_{ssp}(CD_3as)/\chi^{(2)}_{ssp}(CD_3ss)$, and (c) the orientation angle (θ) of carbon chain after adding PBS (0.5 mol/L, 40 μL) into the d_{54}-DMPG bilayer subphase at t=0 min. The solid lines are just used to guide the reader's eyes.

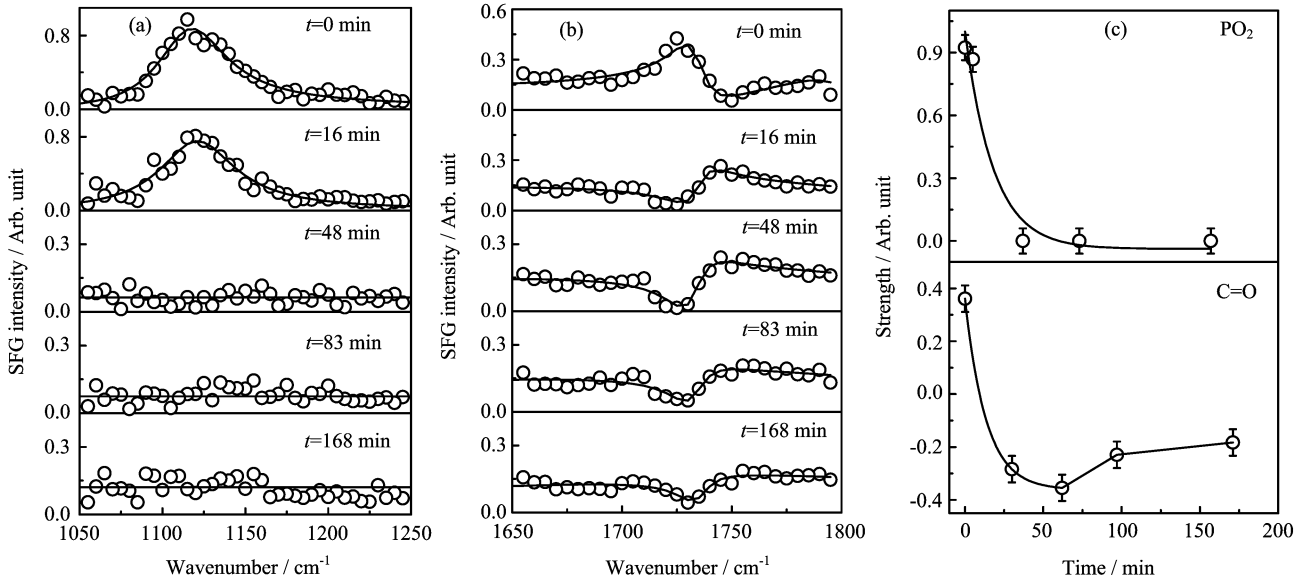

FIG. 4 Time dependence of ssp spectra of lipid bilayer after adding PBS (0.5 mol/L, 40 μL) at t=0 min. (a) Lipid PO_2^- group, (b) Lipid C=O groups and (c) Time dependence of fitting strength of the ssp PO_2^-ss and C=Oss stretching after adding PBS into the d_{54}-DMPG bilayer subphase at t=0 min. Open circles show the experimental data, the solid lines are just used to guide the reader's eyes.

gate the influence of PBS on the head groups by monitoring the spectra of lipid phosphate group and carbonyl group. Figure 4 (a) and (b) show the time-dependent spectra in the frequency range of 1050−1250 cm^{-1} and 1650−1800 cm^{-1} after adding PBS into the d_{54}-DMPG bilayer subphase. The spectra of phosphate group are dominated by the peak at ∼1115 cm^{-1}, which is contributed by PO_2^- symmetric stretch (PO_2^-ss) [27]. The spectra of carbonyl group show a peak at ∼1735 cm^{-1}, which arises from C=O stretch (C=Oss) [46]. A relatively quantitative change of the ∼1115 and ∼1735 cm^{-1} peaks can de deduced by fitting the spectra in Fig.4 (a) and (b) using Eq.(S2) in supplementary material. Their strength change as a function of time is plotted in Fig.4(c). After injecting the salt solution, the intensity of the ∼1115 and ∼1735 cm^{-1} peaks both decreases with time. The ∼1115 cm^{-1} peak completely disappears after t=16 min, while the phase of C=O become negative, indicating that ions can bind not only to phosphate group, but also to carbonyl group. It has been evident that K^+ can penetrate deeply into the bilayer, bind to carbonyl region of lipid molecules and form stable complexes with lipids [6]. In addition, it is believed that the anions with strong hydration ability can increase the competition for the hydration water in the solution, leading to partial dehydration of the cation, which will increase the stickiness of the cation to membrane [47]. Therefore, the large hydration abil-

DOI:10.1063/1674-0068/28/cjcp1504070

TABLE I The fitting phase of $\chi^{(2)}_{\rm NR}$ (nonresonant background), CD_3ss, and H_2O in Fig.2.

t/min	$\chi^{(2)}_{NR}$	CD_3ss	H_2O
0	−	+	+
7	−	+	+
21	+	+	−
35	+	+	−
49	+	+	−
77	+	+	−
122	+	+	−
137	+	+	−
151	+	+	−
165	+	+	−

ity of phosphate ions may promote the penetration of K^+ into cell membrane, even though phosphate can't bind to d_{54}-DMPG bilayer.

C. Salt-induced change in the phase of the nonresonant background and the membrane-bound interfacial water

As indicated in Fig.2, obvious change in the SFG spectral profile is observed between 0 and 21 min. Such different spectral profiles must come from the phase difference. Figure 4 also shows the phase of C=O stretching switches after adding PBS. To confirm this presumption, we carefully fitted the spectra. According to the literature [46], because the symmetric stretch and Fermi resonance modes have the same phase, while symmetric stretch and asymmetric stretch modes have opposite phase, therefore, there are only eight combinations of the phase signs for the $\chi^{(2)}_{\rm NR}$, CD_2ss, CD_3ss, and H_2O. Normally, the interfacial water shows the SFG spectra in the frequency range of 3000−3800 cm^{-1} [48−51]. However, the signal of the membrane-bound water at a charged surface is extraordinarily broad and extends to 1600 cm^{-1} [52]. The right tails of the spectra in Fig.2 come from the water signal. To simplify the fitting, we fixed the water signal at 2500 cm^{-1}. We tried all of the combinations to fit the spectra in Fig.2. But only one combination can give the best fitting. The result is given in Table I. It is clearly seen that nonresonant background and interfacial water both switch their phase between t=7 and 21 min. It is recognized that the phase of interfacial water depends on the surface charge [48]. Before adding PBS, the surface is negative, thus the water adopts hydrogen-up conformation. After adding PBS, the potassium ions can penetrate into d_{54}-DMPG bilayer and make the surface charge become more and more positive, and then result in phase change of interfacial water molecules (*i.e.* hydrogen-down conformation).

The lipid bilayer in the preceding study was prepared in pure water and then PBS was injected into the water subphase (∼2.0 mL) of lipid bilayer. Thus there raises a concern on how the lipid bilayers behave when they were prepared in phosphate buffer solution. To address this concern, we prepared the d_{54}-DMPG bilayer at PBS solution with different ion strength. The ssp spectra in the frequency range of 1950−2300 cm^{-1} are shown in Fig.5. It can also be seen that the SFG spectral profile looks different for the lipid bilayer in DI water and PBS. Phase combination for the ionic strength of 10−20 mmol/L is the same as the preceding result (Table II). However, with the ionic strength increasing (≥40 mmol/L), the phase of nonresonant background switches to the same as the result in DI water (Table II).

TABLE II The fitting phase of $\chi^{(2)}_{\rm NR}$, CD_3ss, and H_2O in the d_{54}-DMPG bilayer in Fig.5.

Ionic strength/(mmol/L)	$\chi^{(2)}_{NR}$	CD_3ss	H_2O
0	−	+	+
10	+	+	−
20	+	+	−
40	−	+	−
80	−	+	−

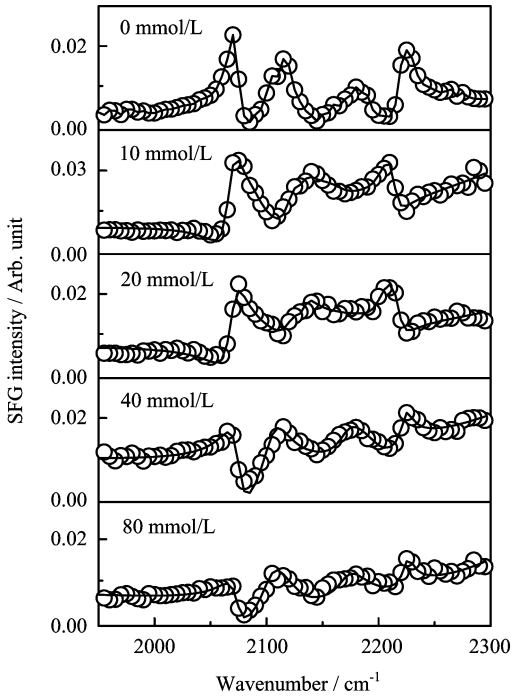

FIG. 5 The ssp spectra of d_{54}-DMPG bilayer in the PBS with different ionic strength. Open circles show the experimental data, solid lines represent the fitting profile.

DOI:10.1063/1674-0068/28/cjcp1504070

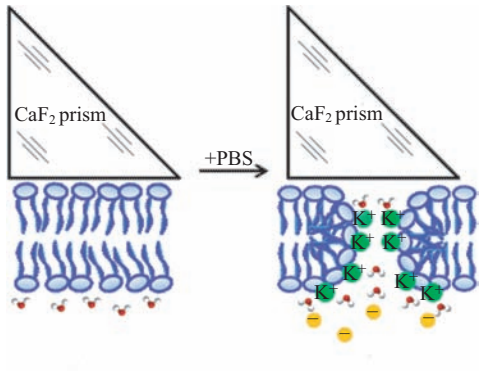

FIG. 6 A scheme of the interactions between potassium PBS and d_{54}-DMPG bialyer.

D. Interaction models of potassium PBS with d_{54}-DMPG bilayer

Currently there are several possible mechanisms of ion permeation across lipid membranes, namely, solubility-diffusion model, transient pore model, and ion-induced defect model [53]. The response of SFG spectra from the tailed and head groups to these models is different. A large signal change from phosphate group, carbonyl groups and alkyl chains of the lipid bilayer will be generated in the ion-induced defect models because the defects can induce the lipid monolayers to bend continuously, and then the phosphate group, carbonyl groups and alkyl chains were distorted, which makes the signal from all of these groups of both leaflets cannot cancel each other. In the pore model, the signal from the alkyl chains cannot be canceled while the signals from the phosphate group and carbonyl groups become smaller (even spectrally invisible). The solubility-diffusion model has an insignificant effect on the SFG intensity change. Furthermore, the solubility-diffusion model has been considered to be impossible because the energy barriers for movement of ions into a hydrophobic environment are too high [54]. In term of the spectral response of these several models, the pore model is the most likely one. According to this information, interaction models of potassium PBS with DMPG lipid bilayer can be described in Fig.6. The formation of pore with the presence of potassium PBS greatly favors the peptide to insert into different kinds of charged (negatively, neutrally, and positively) lipid bilayer and overcome the hydrophobic mismatching effects [19, 20].

IV. CONCLUSION

We have applied SFG-VS to investigate the dynamic process of the interaction between potassium phosphate buffer solution and negative d_{54}-DMPG lipid bilayer in real time. Based on spectral dynamic changes of CD_2, CD_3, lipid head phosphate, and carbonyl groups, we can conclude that K^+ can bind to the cell membrane and cause the signal change of CD_2, CD_3, lipid head phosphate and carbonyl groups quickly. Potassium PBS interacts with lipid bilayers most likely by formation of toroidal pores inside the bilayer matrix. This result can provide a molecular basis for the interpretation of the effect of PBS on the ion-assisted transport of protein across the membrane.

Supplementary material: Fitting of SFG-VS signals, orientation angle of CD_3 structure deduced from SFG are given.

V. ACKNOWLEDGMENTS

This work was supported by the National Natural Science Foundation of China (No.91127042 and No.21473177), the Fundamental Research Funds for the Central Universities (No.2340000064 and No.2030020023), and the Key Research Program of Chinese Academy of Sciences.

[1] M. L. Berkowitz and R. Vácha, Acc. Chem. Res. **45**, 74 (2011).
[2] H. Akutsu and J. Seelig, Biochemistry **20**, 7366 (1981).
[3] J. Seelig, P. M. MacDonald, and P. G. Scherer, Biochemistry **26**, 7535 (1987).
[4] F. S. Sizer, L. A. Piché, E. N. Whitney, and E. Whitney, 2nd Edn., *Nutrition*: *Concepts and Controversies*, Stanford: Cengage Learning, (2010).
[5] A. A. Gurtovenko, J. Chem. Phys. **122**, 244902 (2005).
[6] A. A. Gurtovenko and I. Vattulainen, J. Phys. Chem. B **112**, 1953 (2008).
[7] R. Vácha, S. W. Siu, M. Petrov, R. A. Böckmann, J. Barucha-Kraszewska, P. Jurkiewicz, M. Hof, M. L. Berkowitz, and P. Jungwirth, J. Phys. Chem. A **113**, 7235 (2009).
[8] B. Klasczyk, V. Knecht, R. Lipowsky, and R. Dimova, Langmuir **26**, 18951 (2010).
[9] S. Pokorna, P. Jurkiewicz, L. Cwiklik, M. Vazdar, and M. Hof, Faraday Discuss. **160**, 341 (2013).
[10] M. S. Miettinen, A. A. Gurtovenko, I. Vattulainen, and M. Karttunen, J. Phys. Chem. B **113**, 9226 (2009).
[11] H. I. Petrache, T. Zemb, L. Belloni, and V. A. Parsegian, Proc. Natl. Acad. Sci. USA **103**, 7982 (2006).
[12] R. A. Freitas, *Nanomedicine*, *Volume I*: *Basic Capabilities*. Georgetown, Landes Bioscience, TX, 1(1999).
[13] P. Pradhan, R. Ghose, and M. E. Green, Biochim. Biophys. Acta **1717**, 97 (2005).
[14] M. E. Green, J. Theor. Biol. **233**, 337 (2005).
[15] J. A. Freites, D. J. Tobias, G. von Heijne, and S. H. White, Proc. Natl. Acad. Sci. USA **102**, 15059 (2005).
[16] M. Tang, A. J. Waring, and M. Hong, J. Am. Chem. Soc. **129**, 11438 (2007).

DOI:10.1063/1674-0068/28/cjcp1504070

[17] A. Sukhan and R. E. Hancock, J. Biol. Chem. **271**, 21239 (1996).
[18] S. J. Ye, H. C. Li, F. Wei, J. Jasensky, A. P. Boughton, P. Yang, and Z. Chen, J. Am. Chem. Soc. **134**, 6237 (2012).
[19] F. Wei, S. J. Ye, H. C. Li, and Y. Luo, J. Phys. Chem. C **117**, 11095 (2013).
[20] F. Wei, H. C. Li, and S. J. Ye, J. Phys. Chem. C **117**, 26190 (2013).
[21] S. J. Ye, K. T. Nguyen, S. V. Le Clair, and Z. Chen. J. Struct. Biol. **168**, 61 (2009).
[22] Y. R. Shen, *The Principles of Nonlinear Optics*, New York: Wiley, (1984).
[23] E. T. Castellana and P. S. Cremer, Surf. Sci. Rep. **61**, 429 (2006).
[24] A. G. Lambert, P. B. Davies, and D. J. Neivandt, Appl. Spectrosc. Rev. **40**, 103 (2005).
[25] S. J. Ye, F. Wei, H. C. Li, K. Z. Tian, and Y. Luo, Adv. Protein. Chem. Struct. Bio. **93**, 213 (2013).
[26] S. J. Ye and Y. Luo, Sci. China Chem. **57**, 1646 (2014).
[27] N. N. Casillas-Ituarte, X. Chen, H. Castada, and H. C. Allen, J. Phys. Chem. B **114**, 9485 (2010).
[28] M. D. Unitt and J. L. Harwood, Biochem. J. **228**, 707 (1985).
[29] S. J. Ye, G. M. Liu, H. C. Li, F. G. Chen, and X. W. Wang, Langmuir **28**, 1374 (2012).
[30] S. J. Ye and F. Wei, Analyst **136**, 2489 (2011).
[31] T. M. Uehara, V. S. Marangoni, N. Pasquale, P. B. Miranda, K. B. Lee, and V. Zucolotto, ACS. Appl. Mater. Interfaces **5**, 13063 (2013).
[32] S. Thennarasu, R. Huang, D. K. Lee, P. Yang, L. Maloy, Z. Chen, and A. Ramamoorthy, Biochemistry **49**, 10595 (2010).
[33] X. Chen, J. Wang, C. B. Kristalyn, and Z. Chen, Biophys. J. **93**, 866 (2007).
[34] H. C. Li, S. J. Ye, F. Wei, S. L. Ma, and Y. Luo, Langmuir **28**, 16979 (2012).
[35] W. Sung, D. Kim, and Y. R. Shen, Curr. Appl. Phys. **13**, 619 (2013).
[36] M. R. Watry, T. L. Tarbuck, and G. L. Richmond, J. Phys. Chem. B **107**, 512 (2003).
[37] C. Ohe, Y. Ida, S. Matsumoto, T. Sasaki, Y. Goto, M. Noi, T. Tsurumaru, and K. Itoh, J. Phys. Chem. B **108**, 18081 (2004).
[38] X. Chen and H. C. Allen, J. Phys. Chem. A **113**, 12655 (2009).
[39] K. Z. Tian, H. C. Li, and S. J. Ye, Chin. J. Chem. Phys. **26**, 27 (2013).
[40] S. L. Ma, K. Z. Tian, and S. J. Ye, Sci. China Chem. **58**, 1176 (2015).
[41] B. Gaber, P. Yager, and W. Peticolas, Biophys. J. **22**, 191 (1978).
[42] C. S. C. Yang, L. J. Richter, J. C. Stephenson, and K. A. Briggman, Langmuir **18**, 7549 (2002).
[43] R. Bansil, J. Day, M. Meadows, D. Rice, and E. Oldfield, Biochemistry **19**, 1938 (1980).
[44] Z. Liao and J. E. Pemberton, J. Phys. Chem. A **110**, 13744 (2006).
[45] G. Ma and H. C. Allen, Langmuir **22**, 5341 (2006).
[46] S. L. Ma, H. C. Li, K. Z. Tian, S. J. Ye, and Y. Luo, J. Phys. Chem. Lett. **5**, 419 (2014).
[47] E. Leontidis, M. Christoforou, C. Georgiou, and T. Delclos, Curr. Opin. Colloid Interface Sci. **19**, 2 (2014).
[48] X. Chen, W. Hua, Z. Huang, and H. C. Allen, J. Am. Chem. Soc. **132**, 11336 (2010).
[49] S. Gopalakrishnan, D. Liu, H. C. Allen, M. Kuo, and M. J. Shultz, Chem. Rev. **106**, 1155 (2006).
[50] G. Richmond, Chem. Rev. **102**, 2693 (2002).
[51] Y. R. Shen and V. Ostroverkhov, Chem. Rev. **106**, 1140 (2006).
[52] S. Wolf, E. Freier, Q. Cui, and K. Gerwert, J. Chem. Phys. **141**, 22D524-1 (2014).
[53] I. Vorobyov, T. E. Olson, J. H. Kim, R. E. Koeppe II, O. S. Andersen, and T. W. Allen, Biophys. J. **106**, 586 (2014).
[54] D. W. Deamer and J. Bramhall, Chem. Phys. Lipids **40**, 167 (1986).

DOI:10.1063/1674-0068/28/cjcp1504070